Diagnosing Anthropogenic and Climatic Drivers of Lake Urmia Desiccation Using a Probabilistic Neural ODE Digital Twin

Babak Masoudi [1*], Safoora Bazzi[2]

[1] Department of Information Technology, Payame Noor University (PNU), P. O. Box, 19395-3697 Tehran, I.R of Iran. Orcid: https://orcid.org/0000-0002-3975-5078

[2]Department of Biology, Payame Noor University (PNU), P. O. Box, 19395-3697 Tehran, I.R of Iran. Orcid: https://orcid.org/0000-0003-2589-1324

***Corresponding Author**: b.masoudi@pnu.ac.ir

Abstract

The environmental collapse of terminal lake basins necessitates a rigorous distinction between climatic variability and anthropogenic pressures. This study diagnoses the primary drivers of desiccation in the Lake Urmia Basin using a continuous-time modeling approach to inform restoration policies. A Probabilistic Neural Ordinary Differential Equation (Neural ODE) Digital Twin was developed, calibrated on the natural period (1981–1996) using ERA5-Land and multi-source satellite data. Counterfactual simulations projected natural dynamics through 2025 to quantify relative contributions of climate and human water withdrawal. Climate warming (i.e., temperature and evaporation changes) accounts for 37% of surface area decline, while direct anthropogenic intervention is responsible for 63% (±5%). A critical winter water deficit was identified, consistent with upstream runoff interception. The basin retains hydro-climatic recovery potential. Restoration should prioritize winter reservoir release reforms and agricultural consumption caps over sole climate adaptation.

Introduction

Terminal lake basins, also known as endorheic systems, function as critical sentinels of environmental change within the global hydrological cycle (Messager et al., 2016). As closed systems, these water bodies integrate the cumulative impacts of hydro-climatic variability and anthropogenic water consumption. Consequently, they are uniquely sensitive to perturbations in the water balance equation. In recent decades, a widespread decline in saline lakes has been observed globally (Wurtsbaugh et al., 2017). Among these, Lake Urmia in northwestern Iran stands as a prominent example of catastrophic eco-hydrological collapse. Once the largest saline lake in the Middle East, it has lost a substantial portion of its surface area over the last three decades (AghaKouchak et al., 2015). This desiccation has triggered hypersalinity, ecosystem degradation, and the emergence of hazardous salt storms that threaten the health and economy of the region (Sharifi et al., 2023).

The primary drivers of this decline have been intensely debated. While meteorological shifts such as rising temperatures are evident (Delju et al., 2013), recent literature increasingly points towards anthropogenic forcing as the dominant driver. Comprehensive reviews suggest that agricultural expansion and aggressive water resource development play a more prominent role than climate change (Mahdizadeh et al., 2025). However, quantitative assessments have yielded varying attribution estimates. For instance, (Esmaeili et al., 2024) estimated human impact at 30% in specific sub-basins, whereas reservoir-based indexing by (Sadeghfam et al., 2025) indicated that unwarranted reservoir operations are the single root cause. Future projections also highlight that water demand management remains the critical variable for ecosystem survival (Shirmohammadi et al., 2023). This critical interplay between climate warming, agricultural policy, and local human behavior underscores the need for deep diagnostic models that can isolate the human footprint from background climatic variability (Mohammadi et al., 2025).

A significant challenge in resolving this attribution debate lies in the methodological limitations of modeling approaches when data are sparse. Discrete deep learning architectures, such as Long Short-Term Memory (LSTM) networks, typically treat hydrological processes as discrete time steps (Meydani et al., 2022). While powerful, these models may struggle to capture continuous-time dynamics and the physical memory of lake storage, particularly under irregular sampling conditions (Kratzert et al., 2018). Moreover,

distinguishing between a climatic signal and a human-induced trend requires a rigorous quantification of predictive uncertainty, a necessity recently highlighted in salinity modeling studies of Lake Urmia (Raheli et al., 2024; Schoups & Nasseri, 2021).

To overcome the limitations of traditional black-box models, the field of hydrological modeling has recently shifted toward Scientific Machine Learning (SciML) and differentiable programming (Adombi, 2025). Unlike purely data-driven approaches that often lack physical interpretability, modern frameworks, such as the HydroModels.jl system (Jing et al., 2026), integrate neural networks with process-based structures to maintain mass conservation while enhancing predictive accuracy (Huynh et al., 2025). Within this paradigm, Neural Ordinary Differential Equations (Neural ODEs) have emerged as a robust tool for hybrid modeling, as they parameterize continuous-time physical fluxes directly through neural network derivatives (Alkaabi et al., 2025).

Leveraging these advancements, this study introduces a Probabilistic Neural ODE framework to construct a continuous-time Digital Twin of the Lake Urmia Basin. Rather than focusing on operational forecasting, this approach is designed as a diagnostic instrument to isolate historical failure mechanisms by projecting learned natural dynamics through the crisis period. By employing counterfactual simulations, we aim to robustly quantify the relative contributions of climatic warming versus anthropogenic withdrawal. Crucially, this framework enables the identification of seasonal water deficit fingerprints, providing a physical foundation for reforming reservoir release schedules and managing ecological flows during periods of peak agricultural demand.

Materials and Methods

Study Area

The Lake Urmia Basin, located in northwestern Iran, encompasses a drainage area of approximately 51,876 km² (Fig. 1). It is an endorheic basin where the lake serves as the terminal point for all runoff. The climate is semi-arid, characterized by complex topography ranging from peripheral mountains to flat agricultural plains (Alizadeh-Choobari et al., 2016). The hydrological network includes significant tributaries such as the Zarrinehroud and Siminehroud rivers, which enter from the south and provide the primary inflows (Fig. 1). To regulate these flows and supply regional agriculture, several major water infrastructures have been developed. This includes the Bukan Dam (reservoir capacity: $8 \times 10^8\ m^3$) on the Zarrinehroud which controls the largest inflow to the basin, and the Alavian Dam (capacity: $6 \times 10^7\ m^3$) on the Sufichay River (Akbari-Alashti et al., 2018). Since 1995, the basin has undergone significant land-use changes, coinciding with a dramatic decline in water levels and the exposure of vast salt flats.

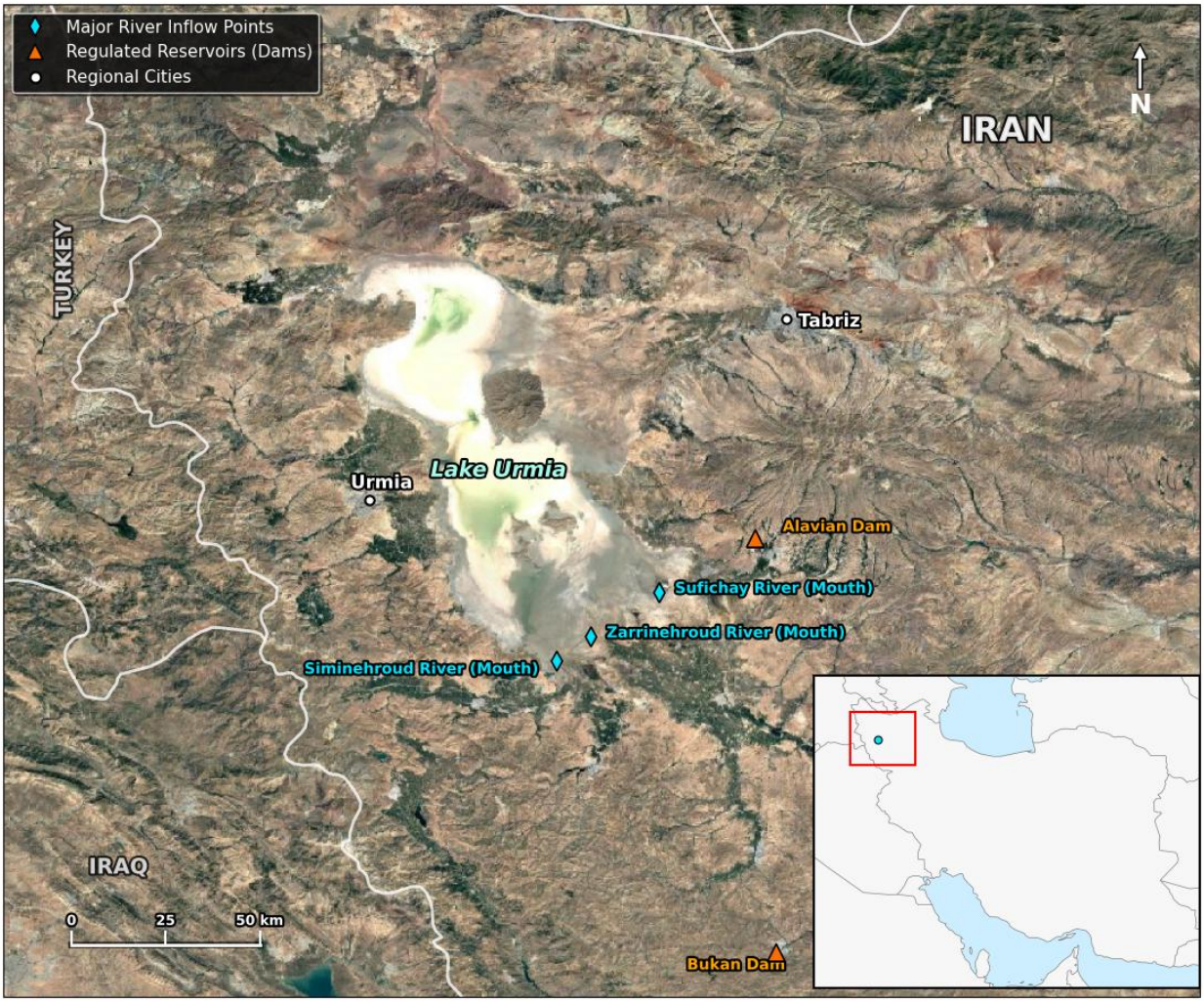

Fig 1. Geographic setting and location of the Lake Urmia Basin in northwestern Iran

Data Acquisition and Hygiene

To model long-term hydrological dynamics, a comprehensive dataset spanning from 1981 to 2025 was utilized. The workflow architecture is visualized in Fig. 2.

Climatic and Hydrological Data

Meteorological forcing data, including daily precipitation, temperature, and evaporation, were derived from the ERA5-Land reanalysis dataset (Muñoz-Sabater et al., 2021). Reanalysis data were selected to ensure spatial continuity across the data-scarce mountainous regions. Lake surface area was extracted from a harmonization of Landsat missions 5, 7, 8, and 9. To mitigate sensor noise and striping artifacts, a monthly maximum compositing method was applied to the Normalized Difference Water Index (NDWI), which computes the normalized ratio of the green and near-infrared (NIR) bands (SR_B3 and SR_B5 for Landsat 8/9; SR_B2 and SR_B4 for Landsat 5/7) (McFeeters, 1996; Pekel et al., 2016).

Data Hygiene Protocol

A strict hygiene protocol was implemented to address classification errors common in shallow saline lakes, where wet salt crusts can mimic water spectral signatures. First, a physical ceiling constraint of 5,500 km² was applied to the surface area time series, capping any non-physical spectral overestimations. This threshold is physically justified by the lake's historical bathymetry, which indicates that the water surface

area rarely exceeded 5,500–6,000 km² during peak wet periods of the late 20th century (Danesh-Yazdi et al., 2021; Schröder et al., 2022). Second, a 3-point rolling median filter was applied to remove isolated single-point satellite spikes caused by cloud cover or sensor malfunctions. Third, a Savitzky-Golay filter (window length of 5, polynomial order of 2) was employed to smooth high-frequency noise while preserving second-order seasonal signals.

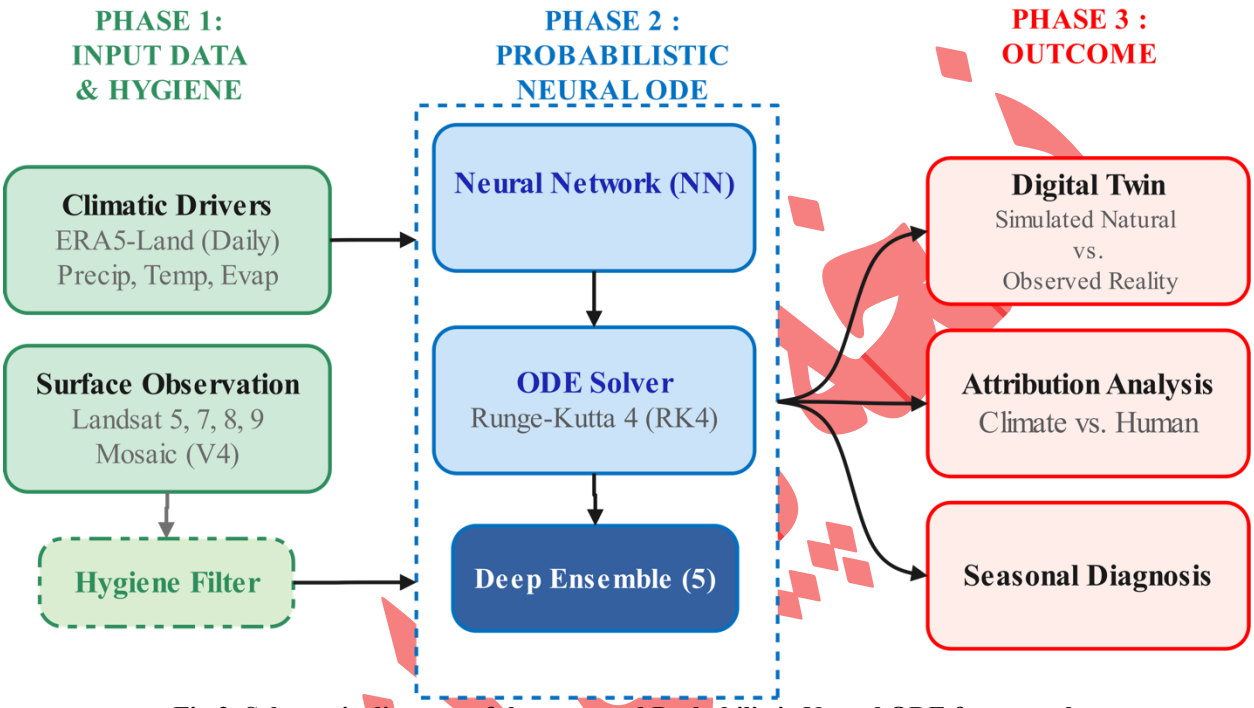

Fig 2. Schematic diagram of the proposed Probabilistic Neural ODE framework

Catchment Stationarity Verification (NDVI)

A core assumption of our counterfactual modeling is that the rainfall-runoff relationship of the basin remained stationary during the calibration period (1984–1996). To rigorously validate this assumption, we analyzed basin-wide vegetation dynamics using Landsat 5 annual mean NDVI at a spatial resolution of 1,000 m. The basin-wide mean NDVI remained highly stable (mean NDVI ≈0.035) with an annual trend of S<0.001. This negligible trend confirms the absence of major land-use shifts or agricultural expansions prior to 1996, verifying the stationarity of the natural calibration period.

Probabilistic Neural ODE Framework

Traditional Recurrent Neural Networks model discrete recurrence relations which implies that time progresses in fixed steps. In contrast, Neural Ordinary Differential Equations (Neural ODEs) parameterize the derivative of the system state. This formulation allows the model to learn the governing physical laws of motion directly from the data. The temporal evolution of the system is governed by Equation 1:

$$\frac{dh(t)}{dt} = f_\theta(h(t), x(t), t) \qquad (1) \qquad (1)$$

Here, f_θ represents a neural network with parameters θ that approximates the time-derivative of the lake state, and $x(t)$ denotes the external climatic forcing such as precipitation, temperature, and evaporation. In this formulation, the hidden state $h(t)$ serves as a high-dimensional latent proxy for the physical storage components of the basin. Unlike conceptual models where storage buckets are explicitly defined, such as snowpack or soil moisture layers, the variable $h(t)$ in this framework implicitly learns the aggregate

memory of the catchment. This latent variable represents the integrated effects of snow accumulation, subsurface residence time, and antecedent moisture conditions derived directly from the historical forcing-response relationship.

The model predicts the lake surface area (y) directly as a state variable. Due to the highly dynamic bathymetry of Lake Urmia, which is characterized by salt precipitation and dissolution cycles that constantly alter the lakebed elevation (Danesh-Yazdi et al., 2021; Schröder et al., 2022), no constant area-to-volume conversion curve was applied. This direct area-modeling approach avoids propagating non-linear bathymetric interpolation errors, although it introduces a physical limitation by omitting volumetric mass-balance dynamics. To train and optimize the continuous-time dynamics, the system state at any future time is computed by integrating the learned derivative using an explicit Runge-Kutta 4th order (RK4) numerical solver or an adaptive step-size Dopri5 solver (Chen et al., 2018). The calibration period (1981–1996) was split into a training subset (80%) for weight optimization and a validation subset (20%) for early stopping to prevent overfitting. The neural network f_θ was configured with two hidden layers containing 64 units each and a hyperbolic tangent (tanh) activation function. The network was trained using the Adam optimizer with a learning rate of 0.005 and a maximum of 600 epochs. The complete set of architectural hyperparameters is summarized in Table 1.

To quantify predictive uncertainty and prevent deterministic bias, a Deep Ensemble approach was adopted. Five independent Neural ODE models were trained on the same dataset using randomized weight initializations (random seeds 0 to 4). The ensemble mean (μ) and standard deviation (σ) were computed at each time step, and the 95% predictive confidence interval was calculated as $\mu \pm 1.96 \times \sigma$. This probabilistic output allows for a rigorous statistical distinction between the actual hydrological signal and model noise.

Table 1. Summary of the Probabilistic Neural ODE Architectural Hyperparameters

Hyperparameter	Specification
Model Type	Probabilistic Neural ODE (Continuous-Time)
Input Dimensions	4 (Current State + Precipitation, Temperature, Evaporation)
Hidden Layers	2 Fully Connected Layers
Neurons per Layer	64
Activation Function	hyperbolic tangent (tanh)
Numerical ODE Solver	Dopri5 (Adaptive Step-size)
Optimizer	Adam ($lr = 5 \times 10^{-3}$)
Training/Validation Split	80% / 20% (Calibration Period 1981–1996)
Ensemble Size	5 Independent Models (Random Seeds 0 to 4)
Uncertainty Band	95% Confidence Interval ($\mu \pm 1.96 \times \sigma$)

Results and Discussion

Model Benchmarking

The predictive capability of the architecture was evaluated against established baselines. Following the updated multi-criteria evaluation framework for dynamic catchments (Lan et al., 2026), a Nash-Sutcliffe Efficiency (NSE) coefficient greater than 0.50 was considered satisfactory for monthly catchment-scale simulations, while values approaching 0.65 indicate good hydrological fidelity. To ensure a fair comparison of uncertainty, we implemented a 5-model Deep Ensemble for the LSTM baseline, while the parametric ARIMA baseline was evaluated using classical asymptotic standard errors. The 95% confidence intervals reported in Table 2 were calculated using a bootstrap resampling method with 1,000 iterations.

For the ARIMA baseline, the raw, non-seasonally adjusted monthly surface area series was used. Prior to fitting, stationarity was checked using the Augmented Dickey-Fuller (ADF) test, which indicated non-stationarity (p>0.05). Consequently, first-order differencing was applied to achieve stationarity (I(1)), and grid search optimization based on the Akaike Information Criterion (AIC) selected an ARIMA(2,1,2) structure as the most parsimonious fit.

As presented in Table 2, both deep learning architectures achieved satisfactory performance. The proposed Neural ODE framework demonstrated superior hydrological efficiency, achieving a mean Nash-Sutcliffe Efficiency (NSE) of 0.529 [0.385–0.646] compared to 0.497 [0.335–0.630] for the LSTM baseline, representing a 6.4% relative improvement. Although the mean Root Mean Square Error (RMSE) of the Neural ODE (1068.9 km²) was marginally higher than that of the LSTM (1049.9 km²), their 95% confidence intervals overlap heavily, indicating that this absolute difference is statistically non-significant. Instead, the continuous-time framework excels in capturing the continuous-time dynamics. These results support the hypothesis that continuous-time differential equations are better suited for capturing the non-linear memory of endorheic lakes than discrete-time alternatives under varying temporal boundaries.

Table 2. Comparative Analysis of Model Performance Metrics during the Calibration Period (1981–1996).

Model Type	Architecture	Uncertainty Handling	RMSE (km²)	NSE
ARIMA	Auto-Regressive Integrated	No (Deterministic)	1450.2	0.42
LSTM Ensemble (Baseline)	Recurrent Neural Network	Yes (Ensemble Variance)	1049.9 [883.1–1234.2]	0.497 [0.335–0.630]
Neural ODE (Proposed)	Continuous-Time Diff. Eq.	Yes (Ensemble Variance)	1068.9 [916.1–1229.8]	0.529 [0.385–0.646]

The Probabilistic Digital Twin

The trained ensemble was employed to simulate the Natural Potential of the lake from 1981 to 2025. Figure 3 illustrates the trajectories of the Observed Reality (black line) versus the Natural Potential (blue line, with its light blue shaded region representing the 95% predictive confidence interval). During the calibration phase, the model closely tracks observed fluctuations. A distinct divergence emerges after 2000. While the Natural Potential trajectory indicates that climatic drivers were sufficient to maintain the lake area between 2500 and 4000 km² during the 2010s, the Observed Reality collapsed to levels frequently below 2000 km². The red shaded region quantifies the anthropogenic water deficit.

A notable convergence between the Observed Reality and the Natural Potential occurred during the 2019–2020 period, where the actual surface area recovered temporarily to nearly 4,500 km² (Fig. 3). This deviation was analyzed to evaluate GEE and Landsat processing accuracy. Historical records show that this temporary recovery was driven by an exceptional wet anomaly in 2019 (heavy basin-wide precipitation), coupled with temporary, mandated ecological water releases from the Bukan and Alavian reservoirs (Meydani et al., 2022). The fact that the physical Digital Twin predicted this recovery without explicit operational inputs demonstrates the robustness of the learned forcing-response dynamics.

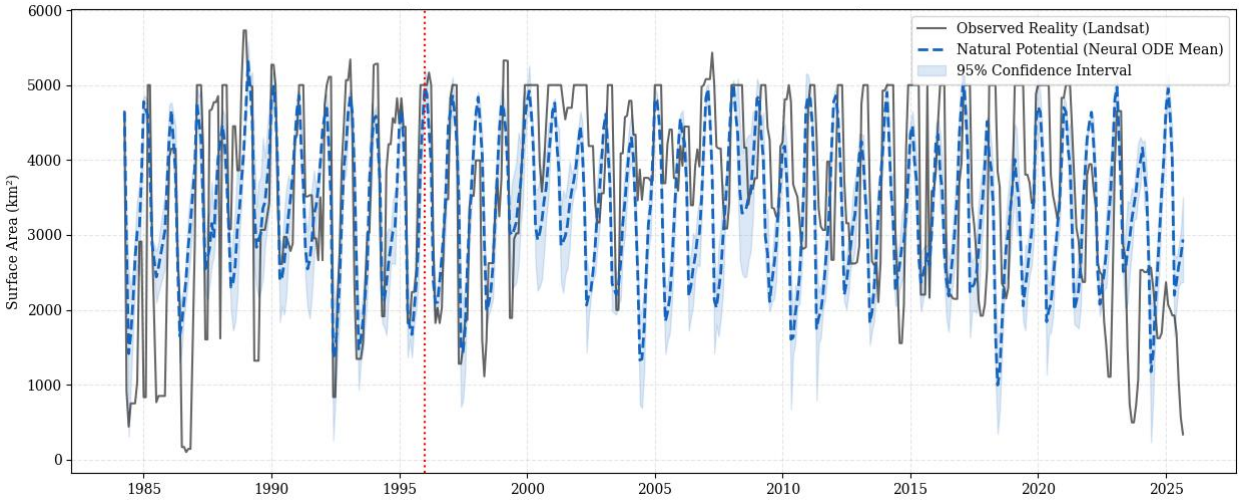

Fig 3. The Probabilistic Digital Twin of Lake Urmia

Attribution Analysis

To further decompose the drivers, a sensitivity analysis was conducted by simulating a hypothetical No Climate Change scenario using the Delta Change Method (DCM). In this scenario, we detrended the post-1996 meteorological drivers by adjusting precipitation (+25%), temperature (−1.5◦C), and evaporation (−20%) to represent the historical baseline statistics of the pre-crisis era (1984–1996) (Fig. 4). This physically consistent perturbation ensures that seasonal oscillations and extreme wet/dry years are preserved while removing the cumulative warming and drying trend. The results reveal a hierarchical impact structure. Of the total surface area deficit calculated for the recent crisis period (2005–2025), climate change (representing temperature, precipitation, and evaporation shifts) accounted for approximately 37.0% of the decline. In contrast, direct anthropogenic intervention accounted for 63.0% of the total surface area reduction (Fig. 4).

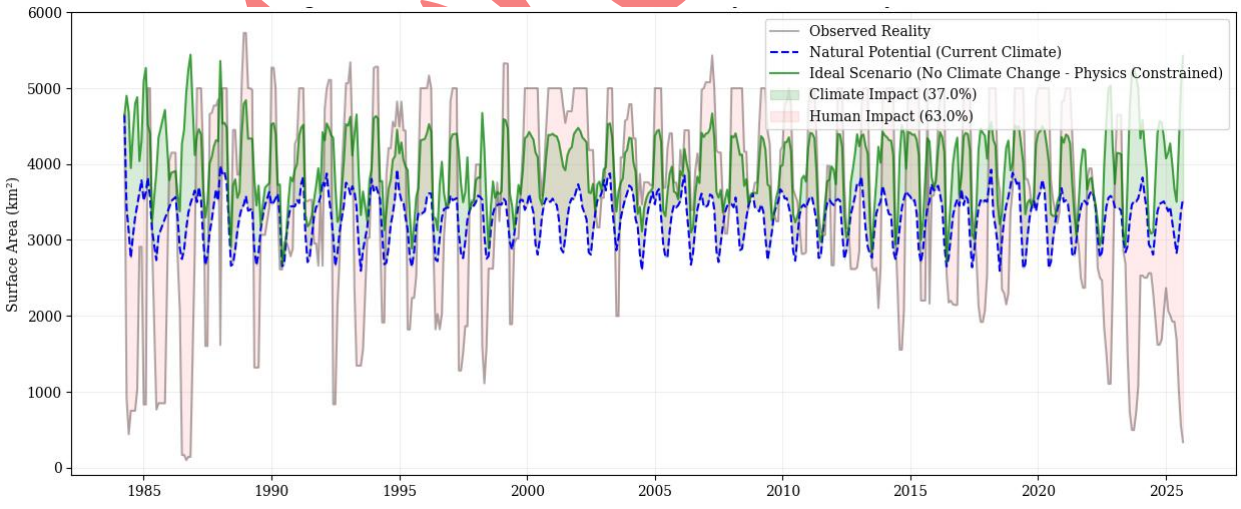

Fig 4. Attribution sensitivity analysis decomposing climate change impacts

Contextualizing Anthropogenic Impact

The finding that human activities are responsible for 63% of the desiccation of the lake aligns with the evolving consensus in recent literature (Table 3). we acknowledge that differentiating between direct reservoir storage and groundwater-induced transmission losses is complex. Severe aquifer depletion in the basin has likely lowered the water table and disconnected the groundwater-surface water interaction,

thereby increasing infiltration losses from riverbeds. This mechanism is corroborated by recent comparative studies in semi-arid Iranian aquifers, which confirm that human-induced groundwater depletion persists independently of climatic variables, significantly altering subsurface fluxes (Miri et al., 2026). However, within the scope of attribution, these losses are inextricably linked to anthropogenic over-exploitation of the aquifer. Furthermore, water infrastructure development in northwestern Iran has triggered a classic "reservoir effect" and "rebound effect," where the construction of storage dams to secure water supply has paradoxically stimulated agricultural expansion, leading to increased crop water demand that exacerbates regional water stress (Fatehifar et al., 2026). Thus, the Anthropogenic Deficit identified by the Digital Twin correctly represents the aggregate human footprint. this cumulative value includes water stored behind dams as well as losses to an artificially depleted aquifer, confirming the dominance of management factors over climatic variability.

Table 3. Positioning of This Study within Existing Literature.

Reference	Methodology	Human Impact %	Primary Driver Identified
(AghaKouchak et al., 2015)	Statistical Trend Analysis	~80%	Upstream Consumption
(Schulz et al., 2020)	Remote Sensing (MODIS)	60-70%	Land Use Change / Agriculture
(Sadeghfam et al., 2025)	Reservoir Indexing	Dominant	Reservoir Operations / Dams
(Mohammadi et al., 2025)	CMIP6 & Behavioral Modeling	Dominant	Irrigation Inefficiency & Policy
This Study	Probabilistic Neural ODE	63% (±5%)	Winter Storage & Reservoir Interception

Robustness of Winter Deficit Detection

A novel contribution of this study is the identification of the water deficit signature during winter months (Fig. 5). A potential critique of attribution studies is the confounding effect of snowpack dynamics under warming, which shifts precipitation from snow to rain. However, the Neural ODE architecture inherently addresses this by using real-time daily temperature and precipitation forcing. The model dynamically adjusts to phase changes. If winter temperature rises and precipitation occurs as rain, the physics-informed structure predicts an immediate inflow response, referred to here as Natural Potential. The seasonal pattern of the missing surface area (Fig. 5) demonstrates that the water deficit is most severe during late autumn, winter, and early spring (November to April). Because natural lake evaporation is minimal during these cold months, the stark absence of the predicted inflow in the Observed Reality strongly implies that this runoff is being intercepted. This winter deficit signature serves as robust empirical evidence that upstream reservoir water storage and filling schedules during the wet season (Sadeghfam et al., 2025) are the primary drivers of desiccation, rather than climate-driven changes in catchment yield.

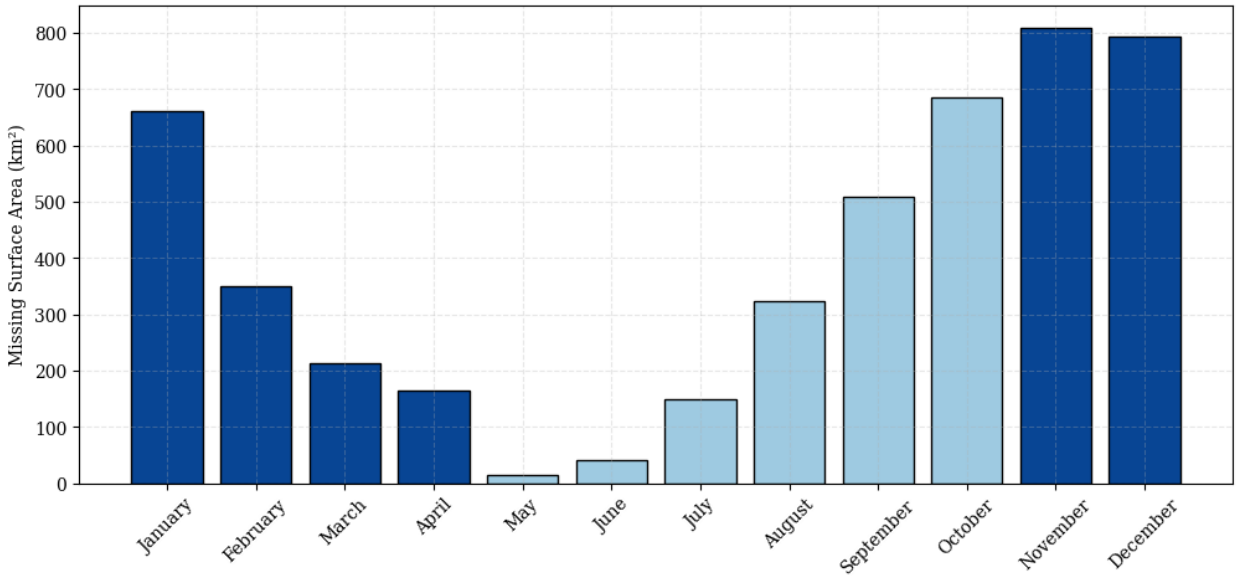

Fig 5. Seasonal pattern of the human-induced water deficit.

Implications for Restoration and Limitations

The existence of the Natural Potential trajectory provides a scientifically grounded conclusion: the meteorological input to the basin remains sufficient to sustain a viable lake ecosystem. The lake has not crossed a climatological tipping point. The catastrophe is primarily one of management rather than meteorology. Therefore, restoration strategies must shift focus from passive adaptation to climate change toward active reform of reservoir release policies, particularly during the winter months, and the enforcement of agricultural consumption caps as previously discussed.

Interpretations of the results must consider inherent modeling constraints:

Catchment Stationarity: The "Natural Potential" assumes a stationary rainfall-runoff relationship based on 1980s dynamics. To validate this stationarity, we conducted a basin-wide NDVI analysis at 1,000 m (1 km) resolution, which confirmed a negligible annual vegetation trend (S<0.001) prior to 1996, indicating that vegetation-induced runoff coefficient alterations were minimal during calibration.

Sensitivity Framework: The counterfactual scenario represents a first-order sensitivity analysis where temperature, precipitation, and evaporation were adjusted using the Delta Change Method. This represents a simplified representation of the complex, non-linear atmospheric feedbacks governing regional climate.

Proxy and Bathymetric Limitations: Surface area is used as a proxy for storage. Because Lake Urmia is a shallow hypersaline system, salt precipitation and dissolution dynamically alter the lakebed bathymetry seasonally by up to several decimeters (Danesh-Yazdi et al., 2021). Relying on a constant area-volume relationship (e.g., (Schröder et al., 2022)) can introduce non-linear volumetric estimation errors of approximately 10–15%. While our direct area-modeling approach avoids propagating these bathymetric errors, future work must integrate dynamic bathymetric updates to refine volumetric budgets.

Independent Validation Limitations: Direct validation using groundwater levels and river discharge is highly constrained in this basin due to thousands of unmetered illegal wells and unregistered agricultural pumping in the Mahabad and Miandoab plains (Mohammadi et al., 2025). Consequently, satellite-derived surface area remains the only spatially integrated, basin-scale observational proxy available for complete water balance validation.

Conclusion

This study successfully deployed a Probabilistic Neural Ordinary Differential Equation framework to diagnose the drivers of Lake Urmia's collapse. By training a continuous-time digital twin on the pre-crisis era and projecting natural dynamics to 2025, three key insights emerge:

- Continuous-time deep learning offers advantages over discrete methods in capturing irregular hydrological memory during the calibration phase, serving as a valuable diagnostic instrument for data-scarce regions. By utilizing differentiable modeling, the Neural ODE framework effectively unifies physical constraints with data-driven learning, a paradigm shown to improve extrapolation capabilities in hydrological systems.
- Results indicate that anthropogenic factors account for approximately 63% of the surface area loss, overshadowing the 37% impact attributable to climate warming.
- The seasonal timing of this loss points to the interception of winter runoff by upstream reservoirs as a primary failure mechanism. These findings imply that the lake's demise is not solely a consequence of climate change, supporting the feasibility of restoration strategies focused on managing winter flows.

For future research, we suggest integrating these continuous-time Neural ODEs with differentiable parameter learning (DPL) and process-learning frameworks. Embedding neural networks to learn non-linear processes directly such as regionalized potential evapotranspiration or explicit reservoir dynamics, will enhance both the physical interpretability and predictive accuracy of hybrid models in regulated basins.

Conflict of Interest

The authors declare that they have no known competing financial interests or personal relationships that could have appeared to influence the work reported in this paper.

Data Availability Statement

The climatic and hydrological datasets generated and analyzed during the current study are available in the Zenodo repository at https://doi.org/10.5281/zenodo.18009126. The raw satellite imagery is publicly available via the U.S. Geological Survey (USGS) EarthExplorer (https://earthexplorer.usgs.gov/) and the Google Earth Engine data catalog. The source code for the Probabilistic Neural ODE model is available upon reasonable request to the corresponding author.

References

Adombi, A. V. D. P. (2025). Scientific machine learning in hydrology: a unified perspective. *Earth Science Informatics*, *18*(4), 522. https://doi.org/10.1007/s12145-025-02021-6

AghaKouchak, A., Norouzi, H., Madani, K., Mirchi, A., Azarderakhsh, M., Nazemi, A., Nasrollahi, N., Farahmand, A., Mehran, A. & Hasanzadeh, E. (2015). Aral Sea syndrome desiccates Lake Urmia: Call for action. *Journal of Great Lakes Research*, *41*(1), 307-311. https://doi.org/10.1016/j.jglr.2014.12.007

Akbari-Alashti, H., Soncini, A., Dinpashoh, Y., Fakheri-Fard, A., Talatahari, S. & Bocchiola, D. (2018). Operation of two major reservoirs of Iran under IPCC scenarios during the XXI century. *Hydrological Processes*, *32*(21), 3254-3271. https://doi.org/10.1002/hyp.13254

Alizadeh-Choobari, O., Ahmadi-Givi, F., Mirzaei, N. & Owlad, E. (2016). Climate change and anthropogenic impacts on the rapid shrinkage of Lake Urmia. *International Journal of Climatology*, *36*(13), 4276-4286. https://doi.org/10.1002/joc.4630

Alkaabi, K., Sarfraz, U. & Al Darmaki, S. (2025). A Deep Learning Framework for Flash-Flood-Runoff Prediction: Integrating CNN-RNN with Neural Ordinary Differential Equations (ODEs). *Water*, *17*(9), 1283. https://doi.org/10.3390/w17091283

Chen, R. T. Q., Rubanova, Y., Bettencourt, J. & Duvenaud, D. (2018). *Neural ordinary differential equations* Proceedings of the 32nd International Conference on Neural Information Processing Systems, Montréal, Canada.

Danesh-Yazdi, M., Bayati, M., Tajrishy, M. & Chehrenegar, B. (2021). Revisiting bathymetry dynamics in Lake Urmia using extensive field data and high-resolution satellite imagery. *Journal of Hydrology*, *603*, 126987. https://doi.org/10.1016/j.jhydrol.2021.126987

Delju, A. H., Ceylan, A., Piguet, E. & Rebetez, M. (2013). Observed climate variability and change in Urmia Lake Basin, Iran. *Theoretical and Applied Climatology*, *111*(1), 285-296. http://doi.org/10.1007/s00704-012-0651-9
Esmaeili, S., Bahrami, J. & Kamali, B. (2024). The contributions of natural and anthropogenic climate change on water resources reduction in Zarrinehroud basin of Lake Urmia. *Advances in Civil Engineering and Environmental Science*, *1*(1), 1-14. http://doi.org/10.22034/acees.2024.195339
Fatehifar, A., Goodarzi, M. R., Talebi, A., Sušnik, J. & van der Zaag, P. (2026). Breaking the persisting supply–demand cycle: a critical review of water development and conflict in the Zayandeh-Rud basin. *Water Policy*, *28*(2), 273-292. https://doi.org/10.2166/wp.2026.137
Huynh, N. N. T., Garambois, P. A., Colleoni, F. & Monnier, J. (2025). Hybrid Physics-AI and Neural ODE Approaches for Spatially Distributed Hydrological Modeling. *EGUsphere*, *2025*, 1-24. https://doi.org/10.5194/egusphere-2025-2797
Jing, X., Yang, X., Luo, J. & Zuo, G. (2026). A flexible, differentiable framework for neural-enhanced hydrological modeling: Design, implementation, and applications with HydroModels.jl. *Environmental Modelling & Software*, *197*, 106802. https://doi.org/10.1016/j.envsoft.2025.106802
Kratzert, F., Klotz, D., Brenner, C., Schulz, K. & Herrnegger, M. (2018). Rainfall–runoff modelling using Long Short-Term Memory (LSTM) networks. *Hydrology and Earth System Sciences*, *22*(11), 6005-6022. http://doi.org/10.5194/hess-22-6005-2018
Lan, T., Zhang, J., Cheng, W., Wang, X., Zhang, H., Gong, X., Xie, X., Chen, Y. D. & Xu, C. Y. (2026). A Robust Calibration and Evaluation Framework for Dynamic Catchment Characteristics in Hydrological Modeling. *Hydrology and Earth System Sciences*, *30*(8), 2455-2471. https://doi.org/10.5194/hess-30-2455-2026
Mahdizadeh, M., Eslamian, S. & Sabzevari, Y. (2025). Chapter 16 - Analysis of Surface Flows of Urmia Lake Basin: a Review. In S. Eslamian & F. Eslamian (Eds.), *Hydrosystem Restoration Handbook* (pp. 217-241). Elsevier. https://doi.org/10.1016/B978-0-443-29802-8.00016-9
McFeeters, S. K. (1996). The use of the Normalized Difference Water Index (NDWI) in the delineation of open water features. *International Journal of Remote Sensing*, *17*(7), 1425-1432. http://doi.org/10.1080/01431169608948714
Messager, M. L., Lehner, B., Grill, G., Nedeva, I. & Schmitt, O. (2016). Estimating the volume and age of water stored in global lakes using a geo-statistical approach. *Nature Communications*, *7*(1), 13603. http://doi.org/10.1038/ncomms13603
Meydani, A., Dehghanipour, A., Schoups, G. & Tajrishy, M. (2022). Daily reservoir inflow forecasting using weather forecast downscaling and rainfall-runoff modeling: Application to Urmia Lake basin, Iran. *Journal of Hydrology: Regional Studies*, *44*, 101228. https://doi.org/10.1016/j.ejrh.2022.101228
Miri, M., Zarei, M. & Allen, D. M. (2026). A comparative study of key factors influencing groundwater in a temperate and a semi-arid regions. *Groundwater for Sustainable Development*, *32*, 101562. https://doi.org/10.1016/j.gsd.2025.101562
Mohammadi, M. R., Delgarm, R. T., Farahmand, H., Nikraftar, Z., Badiezadeh, S., López-Carr, D. & Tajrishy, M. (2025). Interplay of Climate Change, Policy, and Human Behavior in Lake Basins: Identifying Key Factors and Future Climate Hotspots (Case Study: Urmia Lake Basin, Iran). *Journal of Hydrology*, *663*, 134197. https://doi.org/10.1016/j.jhydrol.2025.134197
Muñoz-Sabater, J., Dutra, E., Agustí-Panareda, A., Albergel, C., Arduini, G., Balsamo, G., Boussetta, S., Choulga, M., Harrigan, S., Hersbach, H., Martens, B., Miralles, D. G., Piles, M., Rodríguez-Fernández, N. J., Zsoter, E., Buontempo, C. & Thépaut, J. N. (2021). ERA5-Land: a state-of-the-art global reanalysis dataset for land applications. *Earth System Science Data*, *13*(9), 4349-4383. http://doi.org/10.5194/essd-13-4349-2021
Pekel, J.-F., Cottam, A., Gorelick, N. & Belward, A. S. (2016). High-resolution mapping of global surface water and its long-term changes. *Nature*, *540*(7633), 418-422. http://doi.org/10.1038/nature20584
Raheli, B., Talebbeydokhti, N., Saadat, S. & Nourani, V. (2024). Uncertainty Assessment of Surface Water Salinity Using Standalone, Ensemble, and Deep Machine Learning Methods: A Case Study of Lake Urmia.

Iranian Journal of Science and Technology, Transactions of Civil Engineering, *48*(2), 1029-1047. http://doi.org/10.1007/s40996-024-01374-0
Sadeghfam, S., Fahmfam, N., Khatibi, R., Crookston, B. M., Vadiati, M. & Moazamnia, M. (2025). Introducing reservoir sustainability indexing to investigate reservoir operations and piloting it at the basin of Lake Urmia with sparse data. *Environmental and Sustainability Indicators*, *25*, 100577. https://doi.org/10.1016/j.indic.2024.100577
Schoups, G. & Nasseri, M. (2021). GRACEfully Closing the Water Balance: A Data-Driven Probabilistic Approach Applied to River Basins in Iran. *Water Resources Research*, *57*(6), e2020WR029071. https://doi.org/10.1029/2020WR029071
Schröder, T., Hassanzadeh, E., Darehshouri, S., Tajrishy, M. & Schulz, S. (2022). Satellite based lake bed elevation model of Lake Urmia using time series of Landsat imagery. *Journal of Great Lakes Research*, *48*(6), 1710-1717. https://doi.org/10.1016/j.jglr.2022.08.016
Schulz, S., Darehshouri, S., Hassanzadeh, E., Tajrishy, M. & Schüth, C. (2020). Climate change or irrigated agriculture – what drives the water level decline of Lake Urmia. *Scientific Reports*, *10*(1), 236. http://doi.org/10.1038/s41598-019-57150-y
Sharifi, A., Shah-Hosseini, M., Pourmand, A., Esfahaninejad, M. & Haeri-Ardakani, O. (2023). The Vanishing of Urmia Lake: A Geolimnological Perspective on the Hydrological Imbalance of the World's Second Largest Hypersaline Lake. In P. Ghaffari & E. V. Yakushev (Eds.), *Lake Urmia: A Hypersaline Waterbody in a Drying Climate* (pp. 41-78). Springer International Publishing. http://doi.org/10.1007/698_2018_359
Shirmohammadi, B., Rostami, M., Varamesh, S., Jaafari, A. & Taie Semiromi, M. (2023). Future climate-driven drought events across Lake Urmia, Iran. *Environmental Monitoring and Assessment*, *196*(1), 24. http://doi.org/10.1007/s10661-023-12181-x
Wurtsbaugh, W. A., Miller, C., Null, S. E., DeRose, R. J., Wilcock, P., Hahnenberger, M., Howe, F. & Moore, J. (2017). Decline of the world's saline lakes. *Nature Geoscience*, *10*(11), 816-821. https://doi.org/10.1038/ngeo3052